PREDICTION OF SINGLE-ROTATION PROP-FAN NOISE BY A FREQUENCY DOMAIN SCHEME

H. Gounet and S. Lévy
Office National d'Etudes et de Recherches Aérospatiales,
BP 72, 92322 Châtillon Cedex, FRANCE.

Abstract

The noise of single-rotating propfans is predicted from the solution of the Ffowcs-Williams and Hawkings equation in the frequency domain. The computations under the ICAO certification procedures are based on the concepts developed for conventional propellers, because the flying speeds are low. Emphasis is placed upon noise computation on the fuselage outer wall at cruise speed. Since the helical tip velocities are then transonic, the previous codes must be completed to take into account the non-compactness of the acoustic sources and the blade twist. In addition, a method of estimation of near-field propeller sound levels is developed from the Euler 3D equations. Finally, acoustic measurements on a 1 meter model propfan in the S1-MA transonic wind tunnel of Modane-Avrieux are presented and comparisons with theoretical results are given.

List of symbols

B : number of propeller blades
b : chord at span r
c : sound velocity
D : propeller diameter
F(z) : span force distribution function
f(z,x) : chord force distribution function
h(x) : thickness along the chord
$H(x) = \frac{h(x)}{b}$: reduced thickness
J_{mB} : first kind Bessel function of order mB
l : position along the chord
$M = V/c$: advancing Mach number
$M_{rot} = \frac{\Omega R}{c}$: rotational Mach number at blade tip
$M_{rel} = \sqrt{M_{rot}^2 + M^2}$: relative Mach number at blade tip
m : harmonic order
N : propeller rotational frequency
P : power supplied to the propeller
p : sound pressure
p_t : thickness noise
p_l : loading noise
$R = D/2$: propeller radius
r : position along the span
$S = \sqrt{X^2 + \beta^2 \left(Y^2 + Z^2\right)}$: modified observation distance
V : forward flight speed
(X,Y,Z) : coordinates of observer location
$x = l/b$: reduced chord
$z = r/R$: reduced span (case of a flat blade)
$\beta^2 = 1 - M^2$
ρ : air density
η : propeller efficiency
Ω : rotation speed of propeller
(η_1, η_2, η_3) : point source coordinates.

Introduction

Propfans offer the advantage of a higher propulsive efficiency than turbo-jet engines for flight Mach numbers of 0.7 to 0.8[1,2]. The resulting fuel savings are certain to be of interest for future medium-range airliners. It is for this reason that Aerospatiale, RatierFigeac and ONERA have undertaken, under contract with the French Authorities (DRET, STPA, DPAC), a research program concerning propfan aerodynamics, aeroelasticity and acoustics. This paper refers to the acoustic design of this type of propeller; it is limited to the case of single-rotating propellers and marks a first step before the study of counterrotating propellers and unducted fans, which appear at this time to be among the most probable aircraft solutions.

Propeller pure tone noise prediction codes have been developed at ONERA. Used in former research on propellers for light aircraft[3,4], they were applied to the case of propellers for high-speed aircraft, permitting the calculation of thickness noise and far field loading noise. Section 1 presents the sound level estimates from these programs under the conditions of certification (far field, moderate flying speeds). Section 2 is devoted to the extension of the computations for cruise flight (fuselage noise, high advancing speeds). The improvements provided concern the thickness term which in this case becomes predominant. The non-compactness of the acoustic sources and the blade twist are included in this calculation.

This method, while entirely acceptable under the conditions of certification, is not completely satisfactory in the case of cruising, on the one hand, because the fuselage is located too close to

the propeller to use easily the far field hypotheses and, on the other hand, because the quadrupolar term, which in this case becomes large[5], is not included in the calculations. For these reasons, predictions from aerodynamic calculations based on the Euler 3D equations[6] are currently being developed: the mesh extends only to the vicinity of the blades and the pressure fluctuations, determined only in near field, include all noise sources of aerodynamic origin. This idea, also utilized by Korkan et al.[7], is described in section 3.

Along with the theoretical studies, a 12-bladed propeller model of 1 meter in diameter, was tested in the ONERA S1-MA wind tunnel at Modane-Avrieux. The main objectives were to determine the performance and aerodynamic and aeroelastic characteristics of this model. Acoustic measurements were also carried out and some of the experimental results obtained from these tests are given in section 4.

1. Calculations of the far field type under ICAO conditions of certification

The details concerning the derivation of the expressions and the method used are outlined in[4]. The propeller tone noise sources are broken down conventionally into monopoles (thickness noise), dipoles (loading noise) and quadrupoles. Only the expressions of thickness and loading noise are estalished. To this end, we expand the Lighthill equation in integral form, modified by Goldstein[8] to take into account the motion of translation of the source. The Fourier transform of the expressions leads to making the computations in the frequency domain, which directly gives the sound level of the tones. This method is quite close to that followed by Hanson[9], although the latter is placed straight off in a fixed reference frame, whereas our calculations are worked out in a reference frame linked to the aircraft (origin at the center of the propeller). Likewise, Legendre[10] uses the same basic equations to describe the noise generated by a propeller or by a helicopter rotor, but with respect to a rotating reference frame (linked to the blades). This type of development permits to avoid the singularities which appear at transonic speeds when calculating the solution of the wave equation in the time domain: denominators close to zero can then appear in the source terms. Even so, various means exist to reach the solution[11,12,13].

For calculations under the conditions of certification, the forward velocities and thereby the helical tip velocities are moderate. Some simplifying hypotheses can then be posed. Thus, we consider flat blades and acoustic sources concentrated at one point of the chord, only the span distribution is introduced.

The expressions used in these conditions to describe the sound pressure on the harmonic of order m, at the frequency $f_m = mBN$, are written respectively for the thickness term and the loading term:

$$p_t = -\frac{\rho m^2 B^3 M_{rot}^2 R c^2}{4\pi S\,\beta^4}\left[1+\frac{MX}{S}\right]^2 e^{-\frac{imB\Omega}{c\beta^2}(MX+S)} e^{-imB(\varphi-\pi/2)} \cdot \int_0^1 e^{imB\varphi_0(z)} J_{mB}(mBM_{rot}Az)\left(\frac{b}{R}\right)^2 \int_0^1 x\,H(x)\,dx\,dz \quad (1)$$

$$p_l = \frac{imB\,M_{rot}}{4\pi S\,c}\,\frac{p}{R}\,e^{-\frac{imB\Omega}{c\beta^2}(MX+S)} e^{-imB(\varphi-\pi/2)} \cdot \int_0^1 \int_0^1 \left[\frac{1}{\beta^2}\left(M+\frac{X}{S}\right)\frac{\eta}{M} - \frac{1}{M_{rot}^2 z^2}\right] F_{(z)} f_{(z,x)} J_{mB}(mBM_{rot}Az)\, e^{imB\varphi_0(z)}\,dx\,dz \quad (2)$$

with $A = \sqrt{Y^2+Z^2}/S$ and $\operatorname{tg}\varphi = Z/Y$.

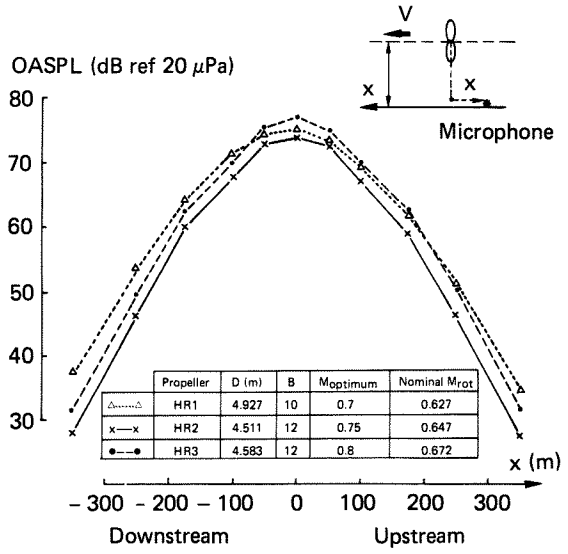

Propeller	D (m)	B	Moptimum	Nominal Mrot
HR1	4.927	10	0.7	0.627
HR2	4.511	12	0.75	0.647
HR3	4.583	12	0.8	0.672

Fig. 1 - Overall sound level variation as a function of observation distance: maximum power 15577 HP - nominal rating - M = 0.3.

Blade dimensions are expressed in reduced coordinates ($x = l/b$ for chord, $z = r/R$ for span); observer location is defined by X, A and φ. Other notations are given at the beginning of the text.

The computer code has been applied to three propellers defined by ONERA for the preliminary aircraft plans of Aerospatiale under certification-type conditions. Figure 1 shows an example of results obtained during a fly-over: we see, in particular, the beneficial effect of a high number of blades.

2. Calculations of the far field type in cruising flight

In the case of cruising flight, the advancing Mach number is of the order of 0.7 to 0.8: the helical tip velocity becomes transonic which generates, a priori, very high noise levels, such as to greatly interfere with the work of the crew and even to cause this type of propulsion to be abandoned for passenger transport, with a fuselage lining which does not add too much to the weight of the aircraft. A sufficiently accurate noise prediction is therefore required. This is the reason why the preceding calculations, drawn up for conventional propellers, must be adapted to take into account the complicated shape of the blades and the non-compactness of the acoustic sources along the chord. It should be mentioned that these modifications have for the time been made only on the thickness term which, at the speeds under study, becomes predominant with respect to loading noise.

2.1 Non-compactness of sources along the chord

We start again by considering flat blades and then introduce the phase shift which exists between two points of the chord $\epsilon(l,r)$: $\operatorname{tg}\epsilon = \frac{l}{r}$ and $\epsilon \sim \operatorname{tg}\epsilon$.

The expression of the thickness noise is then written:

$$p_t = \frac{-i\rho m B^2 M_{rot} RC^2}{4\pi S \beta^2}\left[1 + \frac{MX}{S}\right] e^{-\frac{imB\Omega}{c\beta^2}(MX+S)} e^{-imB\left(\varphi - \frac{\pi}{2}\right)} \cdot \int_0^1 e^{imB\,\varphi_0(z)} \sqrt{M^2 + M_{rot}^2 z^2}\, J_{mB}(mBM_{rot}Az)\left(\frac{b}{R}\right) \int_0^1 H'(x)\, e^{imB\frac{x}{z}\frac{b}{R}}\, dxdz \quad (3)$$

In the case of transonic propellers, the emitted frequencies are such that the wavelengths are comparable to or less than the chord dimension. The phase term $\exp\left(imB\frac{x}{z}\frac{b}{R}\right)$ is other than unity, the acoustic sources radiating at the same time are perceived with a phase shift which tends to partially cancel their contribution. This is expressed (Fig. 2)
by a faster decrease of the sound spectrum with a level on the first acoustic harmonic already lower.

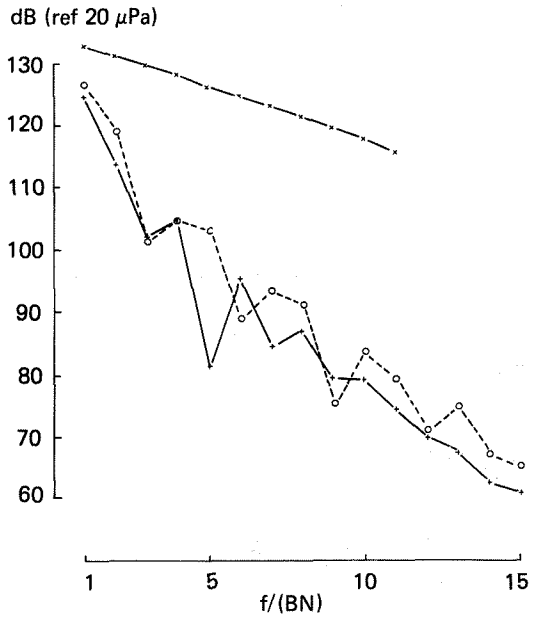

Fig. 2 - Comparison of the various hypotheses of thickness noise computation at transonic speed ($M_{rel} = 0.955$) - Sound spectra in the plane of the propeller at 3.D from the center.
×——× flat blades, compact sources,
○---○ flat blades, non-compact sources,
+——+ twisted blades.

2.2 Introduction of blade twist

The following development permits us to avoid approximations reducing the blades to one plane. Each point of the blade is located in a thee-dimensional space (Fig. 3) and constitutes a sound source whose coordinates are written:

$$\begin{matrix}\eta_1 \\ \eta_2\end{matrix} = \frac{1}{R}\left[\mp\left(1 - \frac{b}{4}\right)\begin{matrix}\sin \\ \cos\end{matrix}(\beta + \varnothing) \mp y_L \begin{matrix}\sin \\ \cos\end{matrix}\varnothing\right]$$

$$\text{and } \eta_3 = \frac{z_L}{R} \quad (4)$$

This code therefore generalises the hypothesis of non-compactness along the chord. The expression for thickness noise takes the following form:

$$p_t = -i^{mB+1}\frac{\rho\, mB^2 M_{rot} Rc^2}{4\pi S \beta^2}$$

$$\int_0^1 \int_0^1 \sqrt{M^2 + M_{rot}^2 r^2}\, J_{mB}(mBM_{rot}A) \left(\frac{b}{R}\right) \frac{H'(x)}{\sqrt{1+H'(x)^2}}$$

$$\left[1 + \frac{M(X-\eta_1 R)}{S}\right] e^{imBM_{rot}A_1} e^{-imB\varphi}\, dxdr \quad (5)$$

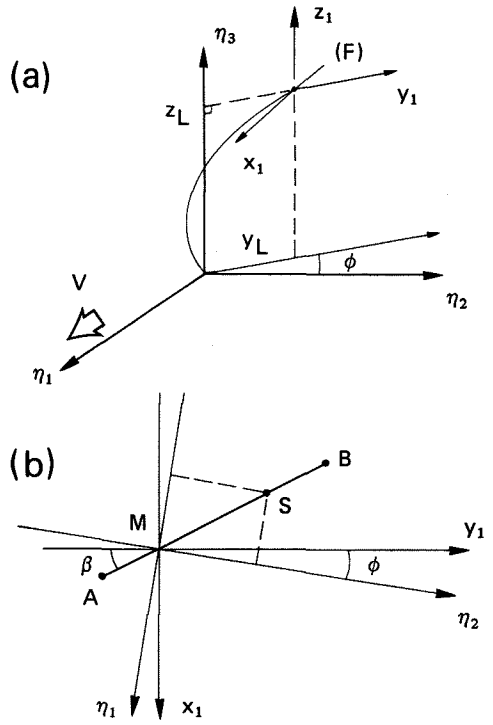

Fig. 3 - Identification of source points S in three-dimensional space.
a) identification of the quarter-chord line F ($M \in F$),
b) view in the plane $\eta_3 = z_L$
AB = length of the chord at position $\eta_3 = z_L$.

with $r^2 = \eta_2^2 + \eta_3^2$

$$A_1 = \eta_1 \left(M + \frac{x}{S}\right) \Big/ \beta^2$$
$$A_2 = (\eta_3 Y - \eta_2 Z)/S$$
$$A_3 = (\eta_2 Y + \eta_3 Z)/S$$

and $A = \sqrt{A_2^2 + A_3^2}$

$tg\ \varphi = A_3/A_2$.

The application of these expressions to the case of a 12-bladed propfan shows that the spectra are entirely comparable to those obtained by the expression (3), if the relative Mach number is subsonic. In the transonic and supersonic domain (Figs. 2 and 4 respectively), differences appear on the spectra. Twist acts like non-compactness of the sources along the chord, by introducing a phase shift between the various points of sound emission. The produced effect depends upon the ratio of the acoustic wavelengths ($\lambda = c/f$) and the characteristic dimensions of a blade; it can go as far as cancellation of certain waves. The result is therefore a reduction of sound levels. The taking into account of blade twist for the calculation of the thickness noise of a propeller in transonic conditions is even more important for observation points located outside the plane of rotation of the propeller (Fig. 5). Thus, for a relative Mach number of 0.955 (case of Fig. 2), the difference on the first acoustic harmonic between the flat-blade and twisted-blade computations changes from 1 dB in the plane of rotation to 4 dB for an observation angle of 60°. The differences can be much greater on the second harmonic.

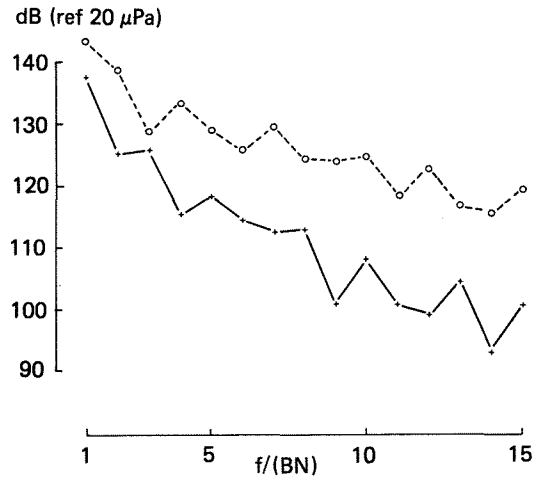

Fig. 4 - Comparison of computations for flat blades and twisted blades at supersonic speed ($M_{rel} = 1.06$) sound spectra in the propeller plane at 3.D from the center.
o----o flat blades
+——+ twisted blades.

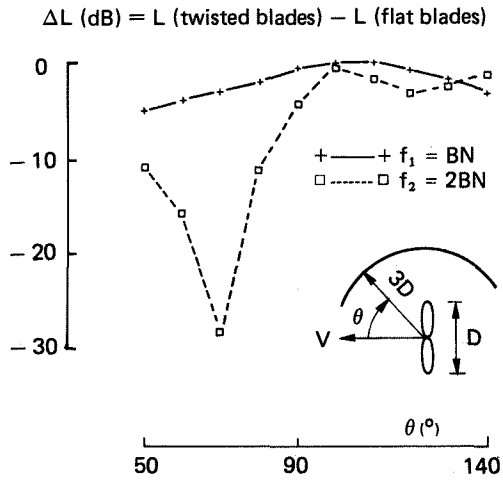

Fig. 5 - Effect of blade twist on the directivity of propeller noise.
B = 12 - $M_{rel} = 0.955$.

The comparisons (Fig. 6) made between the computation of thickness noise (4) with twisted blades and the theoretical and experimental results published by NASA[14] are encouraging. In fact, the computation developed at ONERA and the US computation give similar variations of the sound level of the first acoustic harmonic as a function of the relative Mach number. For relative Mach numbers of less than 1.1, the experimental levels lie within the two types of computations. It should be noted that the observed differences could come, on the one hand, from inaccuracies in the input geometry of the propeller for the ONERA computation (US propeller SR1 with 8 blades) and, on the other hand, from a slight influence of loading noise which is taken into account in the NASA computation.

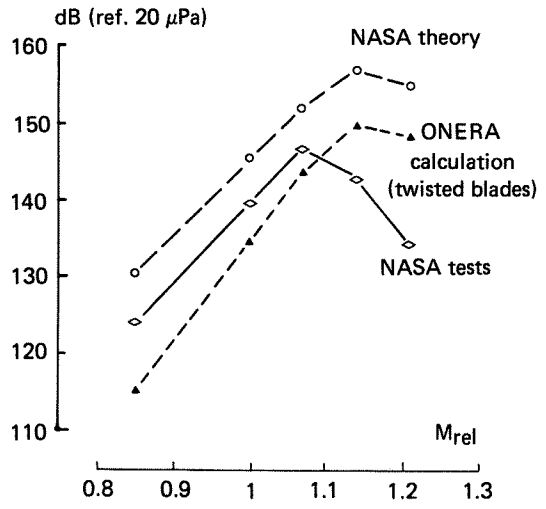

Fig. 6 - Noise level of first acoustic harmonic of the US propeller SR1 in the plane of rotation (B = 8).

3. Near field computations for cruising flight

In order to obtain information concerning noise at the level of the fuselage, which is located at the limit of the far field of the propeller and sometimes even below, ONERA is presently investigating predictions on aerodynamic computations based on the Euler 3D equations[6]: pressure fluctuations are determined on and in the vicinity of the blade. They include all noise sources of aerodynamic origin and thus permit access to the total sound level in the near field of the propeller: not only are the monopole and dipole terms taken into account, but also noise of quadrupolar origin disregarded in the computations presented in preceding paragraphs.

3.1 Sound field computation

The field of pressure fluctuations p_j is obtained by solving the Euler equations by a pseudo-unsteady method. For this purpose, a three-dimensional mesh is used on and near the blade.

For the acoustic computations, we consider only the points located beyond the radius of the blades. The angular distribution of pressure p_j (j from j_{min} to j_{max}) being known over an arc of circle of $2\pi/B$ at a given axial position X and distance d to the axis, its average value ($\bar{p} = \frac{1}{N}\sum_j p_j$ with $N = j_{MAX} - j_{MIN}$) is computed and then the discrete Fourier transform of the function $p(j) = p_j - \bar{p}$. The obtained spectrum p_m ($m = 1,\ldots \frac{N-1}{2}$) describes the acoustic pressure of the harmonics of the propeller noise:

$$\text{at } f_m = mBN,\ L_m = 10 \log_{10} \frac{|p_m|^2}{p_{ref}^2} \text{ with } p_{ref} = 20\ \mu Pa$$

and the overall sound level is obtained by:

$$L(dB) = 10 \log_{10} \frac{p_{rms}^2}{p_{ref}^2} \text{ with } p_{rms}^2 = \sum_{m=1}^{(N-1)/2} |p_m|^2.$$

3.2 Results obtained

The variation of the sound field, for observation points located on a line parallel to the axis of rotation of the propeller, gives information on the fuselage located at a distance d from the propeller axis. It is observed that the sound level is not maximum in the plane of the propeller (X = 0) but slightly downstream. In the example of Figure 7 (d = 1.45 R), the maximum sound emission angle is of the order of 100°. The sound level decreases very rapidly at both sides of this location, because the effects of distance and directivity are combined. The obtained spectra show a very strong dominance of the first acoustic harmonic: whatever the case examined (speed, point of observation), the difference between the first acoustic harmonic and the second harmonic is greater than 10 dB.

The idea to use the aerodynamic results of the Euler computation to evaluate sound levels is also used to advantage by Korkan et al[7]. Figure 8 shows a comparison of the acoustic results as a function of the distance d, in the plane of the SR3 8-bladed propeller. The lack of common parameters concerning propeller geometry as well as power and advancing coefficient explains the bars on our results and makes the comparisons more qualitative than quantitative. We note however that the sound levels are of the same order of magnitude and that the decrease of the field with distance is similar: the sound pressure varies at about $1/d^5$ (attenuation of about 30 dB when the distance is doubled) instead of 1/d in far field. It is planned to

extend the computation to observation distances farther away in order to examine the changes in the rate of decrease and to look for an overlapping with the far field computations. In fact, tests of the SR6 propeller in the Boeing transonic wind tunnel[15] showed that the far field hypotheses are valid whenever the distance d reaches about one or one and a half times the propeller diameter.

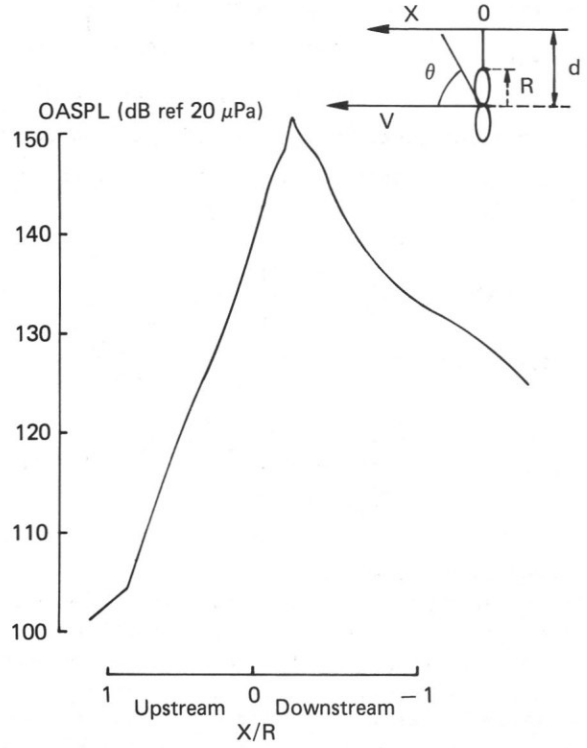

Fig. 7 - Variation of sound level at the frequency f_1 = BN obtained in near field.
B = 12 - d/R = 1.45 - M_{rel} = 1.06.

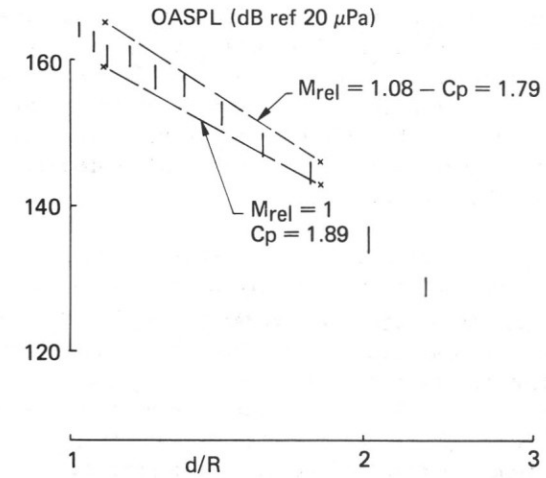

Fig. 8 - Computation of near field sound level in the plane of the SR3 propeller (B = 8).
× Korkan et al.[7] results
Advance ratio J = 3.06.
| ONERA results M_{rel} = 1.06 -
Advance ratio J = 3.15
Power coefficient $1.81 < C_p < 2.18$.

4. Test at S1-MA

In October and November of 1985, the testing of a 12-bladed propfan model, 1 m in diameter, was carried out in the ONERA S1-MA wind tunnel in Modane-Avrieux (return-flow transonic wind tunnel with a closed test section of 8 m in diameter). The propfan (Fig. 9), defined by the ONERA Aerodynamics Department, manufactured and equipped with Kulite pressure transducers by the Helicopter Division of Aerospatiale, was driven by a motor designed and produced by the Large Testing Facilities Department of ONERA and by Ratier-Figeac.

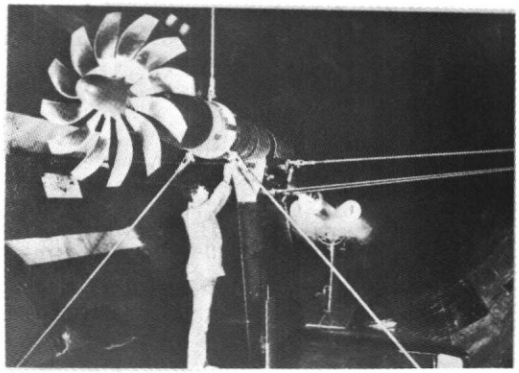

Fig. 9 - Assembly view of propfan model set-up in the test section of the S1-MA wind tunnel.

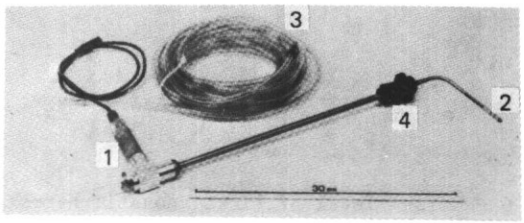

Fig.10 - View of microphone probe for high speed flow.
1 - microphone and adapter Brüel et Kjaer
2 - static pressure tube
3 - anti-reflection coiled tube
4 - wall-mounting clip

Along with the measurements of the propfan performance and blade distortion, which constituted the main objective of this programme, acoustic measurements were taken, in spite of the absence of acoustic lining on the walls of the test section.

4.1 Description of acoustic measurements

The axis of the propfan was located 1.20 m below that of the test section. This off-centre position of the propfan is advantageous for acoustic measurements because it prevents the refocusing of the sound waves on the source, which might occur without acoustic lining.

The main problem encountered in the preparation of these tests was to make suitable acoustic measurements at high velocity, up to a Mach number of 0.75. Three microphones were placed at the wall of the test section, but the acoustic waves risk being disturbed crossing the boundary layer[16]. In order to put the transducers closer to the model, we used waveguide probes (Fig. 10), inspired by those developed for lower speeds by the Acoustics Department of SNECMA, for its studies of propagation in turbo-jet ducts. A probe of this type was placed near a flushmounted transducer, but with the pressure tube outside the boundary layer, in order to assess the effect of the boundary layer and of reflections on the walls. Six other probes mounted in streamlined masts were positioned in the flow at various distances from the propfan and several angular locations. The microphone closest to the propfan is at d = 1.6 m from the center (thus 1.6 diameter). So it is agreed that the ten microphones are in far field with respect to the acoustic source[15].

The tests were carried out for flow Mach numbers between 0.25 and 0.75, without any propeller incidence.

4.2 Behaviour of the obtained results

The signals recorded with a bandwidth of 0 to 20 kHz are analysed with a frequency resolution of 25 Hz; the spectra are plotted in the 0-10 kHz band.

Overall, whatever the flow speed and microphone considered, the propeller pure tones emerge from the broadband noise. For the lowest flow speeds ($M \leq 0.6$), besides the propeller pure tones, tones appear on the spectra (Fig. 11) due to the presence of shrouds visible on Figure 9; these tones actually have a frequency proportional to the flow speed. At M = 0.5, the analysis of the spectra is rendered difficult by the presence of these tones: the first harmonic, at f_1 = BN is very close to the tone due to the shroud of 35 mm in diameter and its sound level is lower. At the highest speeds ($M > 0.6$), the tones due to the presence of the shrouds are buried in the broadband noise (Fig. 12) and, in spite of the very strong increase if the latter) ($\sim$ + 20 dB between M = 0.25 and M = 0.75), the propeller pure tones, or at least the first acoustic harmonic, emerge clearly.

In addition, we observe that, at least on the first acoustic harmonic at f_1 = BN $\simeq$ 1 kHz, the signals picked by the flush-mounted transducers do not seem to be affected by the boundary layer and that the probe near the wall does not appear to be disturbed by reflection phenomena. The difference in sound level on this tone f_1 = BN is of the order of 6 dB, which corresponds to the doubling expected from the sound pressure on a wall. These conclusions concerning reflection, drawn from microphones located in the plane of the propeller, should be moderated for measurements rather distant upstream or downstream, as mentioned in the following paragraph. In addition, a confinement effect is visible in some cases, because microphones farther away from the propeller can perceive more noise than others closer to it.

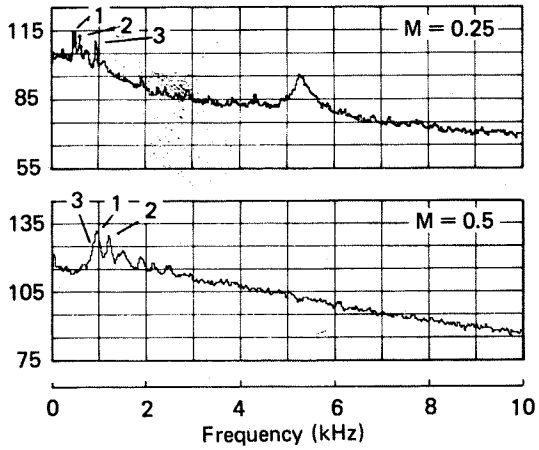

Fig.11 - Spectra obtained at low speed - microphone in the propeller plane at d = 3.5 m.
1 - shroud ø = 35 mm
2 - shroud ø = 30 mm
3 - first harmonic f_1 = BN.

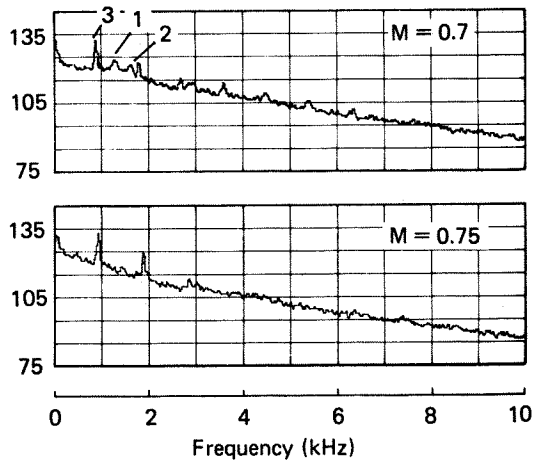

Fig.12 - Spectrum obtained at high speed microphone in the propeller plane at d = 3.5 m.
1 - shroud ø = 35 mm
2 - shroud ø = 30 mm
3 - first harmonic f_1 = BN.

4.3 Preliminary comparisons with theoretical results

For these first comparisons, we used the computational model of the far-field type, with the hypotheses of flat blades and non-compact sources, which takes into account the thickness and average loading noise (expressions 2 and 3). The compari-

sons concern only the sound levels at the first acoustic harmonic frequency $f_1 = BN$ (Fig. 13):

- for microphones located in the plane of the propeller ($\theta = 90°$), the computation and the corresponding test are in good agreement except at maximum speed ($M_{rel} \approx 1.04$) where the theory much overestimates the sound levels; the model taking into account the twisted shape of the blades would lead to a decrease of sound levels and therefore improve the agreement with the experimental results at relative transonic speeds;

- for the microphones placed rather far away upstream and downstream from the plane of the propeller, very large differences appear between the theoretical and experimental results; the computed sound levels are always clearly lower. An explanation, at least partial, may lie in the absence of acoustic lining: since sound emission is maximum around the plane of the propeller, the wall reflections can produce an appreciable increase in the noise perceived upstream and downstream.

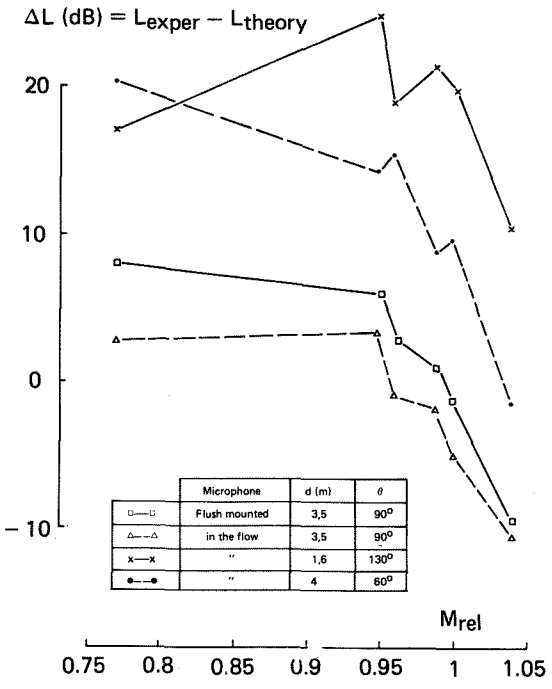

Fig.13 - Comparison of experimental and theoretical results at the frequency $f_1 = BN$.

5. Conclusion

Within the framework of research on propfans carried out in France for several years, the acoustic study of this type of propeller was undertaken. The application of the propeller noise prediction code, developed for conventional propellers, has served to estimate sound levels radiated by three propfans under conditions of certification (low speeds, far field). These data are used by Aerospatiale for aircraft preliminary plans.

In the case of cruising flight in which relative blade-tip velocities become transonic, the farfield noise computations have been improved to take into account the exact shape of the blades and the distribution of acoustic sources along the chord. These modifications are appreciable when the acoustic wavelengths become comparable to the blade dimensions; the phase shifts created are then important and some waves can be practically cancelled. This results in lower sound levels and a spectrum decrease more substantial than in the case of the simplified computation. The work carried out on thickness noise will be extended to the computation of loading noise: if the latter is low for single-rotating propellers in cruising flight, it increases for counter-rotating propellers and unducted fans on account of fluctuations due to the interactions.

In order to be able to obtain near field information including all of the sources of aerodynamic noise, acoustic computations are carried out based on the pressure fluctuations given by the solution of the Euler 3D equations. In the vicinity of the blades, the sound level is maximum for an observation position located slightly downstream from the plane of rotation of the propeller. The rate of decrease of sound pressure with distance is much higher than in far field since an attenuation of 30 dB is observed when the observation distance is doubled, instead of 6 dB in far field. This first study will be followed up mainly by extending the mesh in order to be able to make the connection between near field and far field.

Tests of a transonic propfan model in the S1-MA wind tunnel have permitted a data base on this type of propeller to be constituted. In spite of the differences with theoretical results, due especially to the absence of acoustic lining on the walls of the wind tunnel, the first comparisons are encouraging and new tests with propeller incidence and at higher flow speeds (M = 0.8) are also planned.

Acknowledgements

This study is carried out under contract with the Direction des Recherches, Etudes et Techniques (DRET). The authors would like to express their thanks to the Aerodynamics Department of ONERA for the support offered for this work, and especially to J.M. Bousquet who directs the engineering studies of ONERA on propfans and who executed the Euler computations used for near-field noise prediction.

REFERENCES

[1] J.M. Bousquet, *Hélices pour vol économique à grandes vitesses*, l'Aéronautique et l'Astronautique, n° 88, pp. 37-51, 1981-3.

[2] W.E. Arndt, *Propfans go full scale*, Aerospace America, pp. 100-103, Jan. 1984.

[3] C. Dahan, *Propeller light aircraft noise at discrete frequencies*, AIAA Paper 80-0997, June 1980.

[4] H. Gounet, *Contribution to the study of light aircraft propeller noise*, ONERA, NT 1982-8.

[5] D.B. Hanson, M.R. Fink, *The importance of quadrupole sources prediction of transonic tip speed propeller noise*, J. Sound Vib., **62**, 1, pp. 19-38, Janv. 1979.

[6] J.M. Bousquet, *Aerodynamic methods used in France for designing advanced high-speed propellers*, AGARD CPP n° 366, Ref. 2, Oct. 1984.

[7] K.D. Korkan, E. Von Lavante, *An alternative method of calculating propeller noise generated at transonic tip speeds, including non-linear effects*, AIAA Paper n° 85-0002, Jan. 1985.

[8] M.E. Goldstein, *Aeroacoustics*, Mc Graw Hill Intern. Book Company, New York, 1976.

[9] D.B. Hanson, *Influence of propeller design parameters on far field harmonic noise in forward flight*, AIAA Paper n° 79-0609, March 1979.

[10] R. Legendre, *Noise generated by a propeller or a helicopter rotor*, La Recherche Aérospatiale n° 1982-3, pp. 1-5 (English Edition), May-June 1982.

[11] F. Farassat, G.P. Succi, *A review of propeller discrete frequency noise prediction technology with emphasis on two current methods for time domain calculations*, J. Sound Vib., **71**, 3, pp. 399-419, Aug. 1980).

[12] S.L. Padula, P.J.W. Block, *Acoustic prediction methods for the NASA generalized advanced propeller analysis system (GAPAS)*, AIAA Paper n° 84-2243, July 1984.

[13] A. Azuma, P. Kawachi, T. Watanabe, Y. Nakamura, *Performance and noise analysis of advanced turboprop*, 11th European Rotorcraft Forum, Paper n° 11, Sept. 1985.

[14] J.H. Dittmar, *A comparison between an existing propeller noise theory and wind tunnel data*, NASA TM 81519, 1980.

[15] B.M. Glover, *Noise testing of an advanced design propeller in the Boeing transonic wind tunnel with and without test section acoustic treatment*, AIAA Paper n° 84-2366, Oct. 1984.

[16] J.H. Dittmar, *Experimental investigation of the effect of boundary layer refraction on the noise from high speed propeller*, NASA TM 83764, Sept. 1984.